ChemComm

COMMUNICATION

View Article Online
View Journal | View Issue

Cite this: *Chem. Commun.*, 2021, **57**, 1494

Received 12th November 2020,
Accepted 23rd December 2020

DOI: 10.1039/d0cc07440c

rsc.li/chemcomm

Theoretical evaluation of the carbene-based site-selectivity in gold(III)-catalyzed annulations of alkynes with anthranils†

Kaifeng Wang,[a] Qiao Wu,[a] Siwei Bi,*[a] Lingjun Liu,[a] Guang Chen,[ab] Yulin Li,[c] Tony D. James*[de] and Yuxia Liu*[a]

The gold(III)-catalyzed annulations of alkynes with anthranils were evaluated using DFT calculations. A unified rationale for the Br-migration on α-imino gold(III)-carbene was proposed, from which an unprecedented "N-donation/abstraction substitution" mechanism was established using the substituted anthranils, while direct C–H nucleophilic attack was involved with the unsubstituted anthranils. The controlling factors guiding the site-selectivity were uncovered. These computational studies provide insight for developing new α-imino gold(III)-carbene mediated reactions.

Gold(III)-catalyzed annulations of alkynes[1] with isoxazole derivatives have attracted significant interest since they provide atom- and step-economical access to diverse aza-heterocycles found in numerous natural products, organic functional materials and pharmaceuticals.[2] Considerable effort has been devoted to developing gold carbene-promoted reactions[3] for the selective synthesis of azaheterocyclic scaffolds. In this context, three fascinating annulations have recently been developed by the group of Hashmi to construct diverse azacycles through the tuning of nucleophilic sites for gold(III) carbenoid intermediates (Scheme 1)[4,5] Using $KAuBr_4$ as a catalyst, the reaction of substituted-anthranil **2M** with *N*-benzyl ynamide **1a** is proposed to undergo C^a-nucleophilic attack to generate the quinoline-fused polyazaheterocycle $\mathbf{P_a}$ (Scheme 1(1)),[4] while with *N*-furanylmethyl ynamide **1b** undergoes exclusive C^b-attack, producing 2-amino-pyrrole $\mathbf{P_b}$ (Scheme 1(2)).[4] Interestingly, the annulation of unsubstituted-anthranil **2N** with ynamide **1t** under $AuBr_3$ catalysis, results in the formation of the unprotected 7-acylindole $\mathbf{P_t}$, where C^t attack is favoured (Scheme 1(3)).[5]

The divergence of the nucleophilic site-selectivity at the gold carbene[3] is very interesting but means that access to desired azaheterocycles in a facile and general pattern is challenging. Hence, we decided that it was important to provide an in-depth understanding of the reaction mechanisms and, especially, the inherent origins of the site-selectivity, in order to help generalize these reactions and make them predictable. Mechanistically, according to the general proposal,[6] the reactions in Scheme 1 are assumed to proceed *via* a direct nucleophilic attack of the C^a, C^b or C^t atom at the carbene C atom. By employing an exhaustive DFT evaluation (see the Computational details in the ESI†), we explored whether the direct attack pathway or other alternative mechanisms could be used to rationalize the observed annulation products. Furthermore, the inherent controlling factors

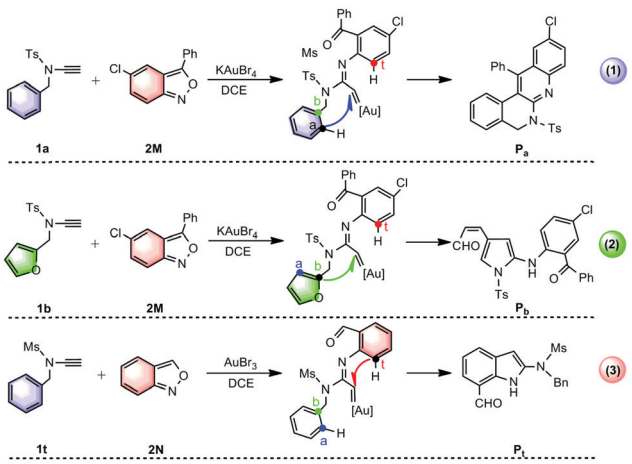

Scheme 1 Gold(III)-catalyzed annulations of *N*-aryl ynamides with anthranils reported by Hashmi's group.[4,5]

[a] *School of Chemistry and Chemical Engineering, Qufu Normal University, Qufu, 273165, P. R. China. E-mail: liuyuxia2008@163.com, siweibi@126.com; Fax: +86-537-4456305; Tel: +86-537-4458308*
[b] *Ministry of Education, Key Laboratory of Hainan Trauma and Disaster Rescue, College of Emergency and Trauma, Hainan Medical University, Haikou 571199, China*
[c] *Key Laboratory of Tibetan Medicine Research & Qinghai Key Laboratory of Qinghai-Tibet Plateau Biological Resources, Northwest Institute of Plateau Biology, Chinese Academy of Science, Xining 810001, Qinghai, P. R. China*
[d] *Department of Chemistry, University of Bath, Bath, UK BA2 7AY, UK*
[e] *School of Chemistry and Chemical Engineering, Henan Normal University, Xinxiang 453007, P. R. China*

† Electronic supplementary information (ESI) available. See DOI: 10.1039/d0cc07440c

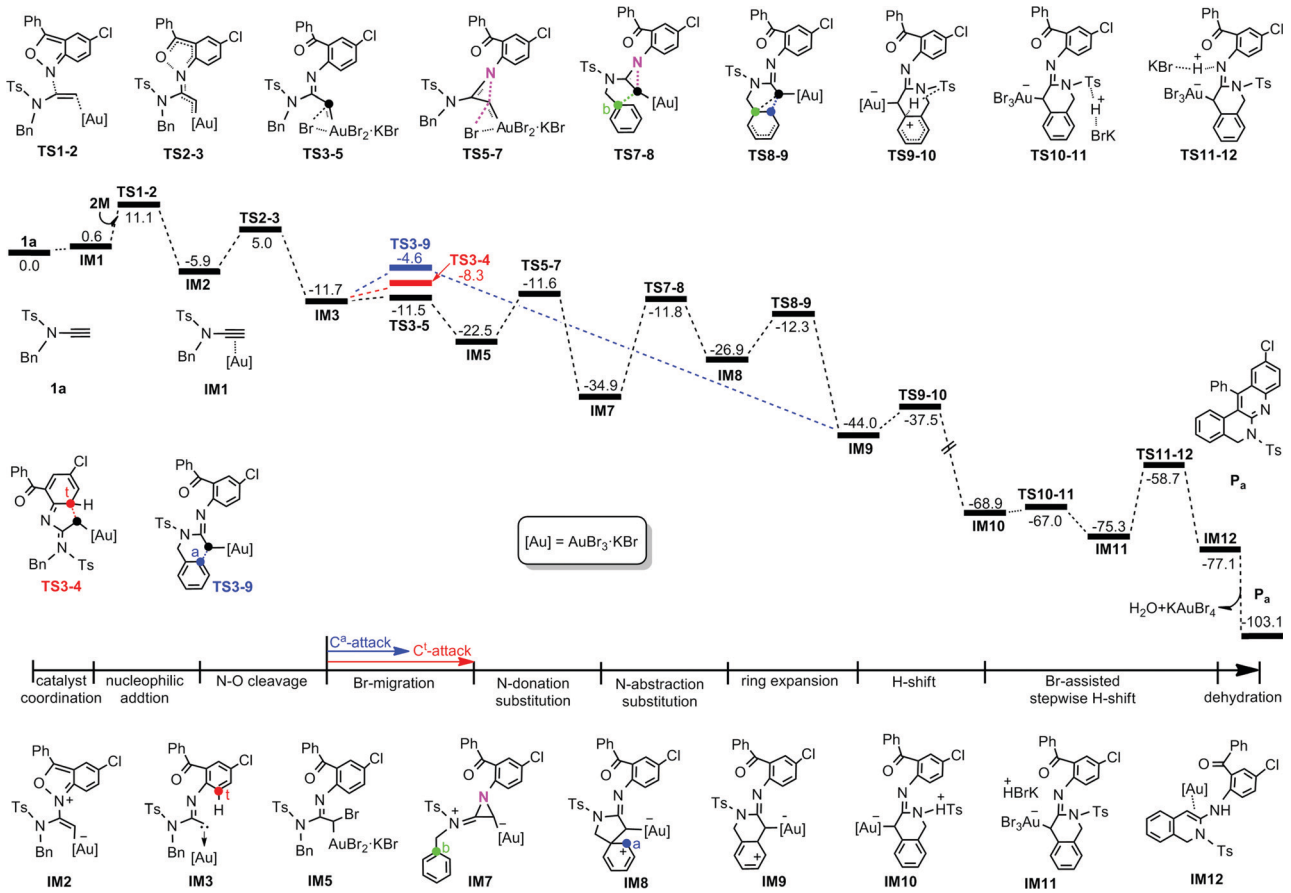

Fig. 1 Calculated Gibbs energy profile in DCE for the formation of quinoline-fused polyazaheterocycle $\mathbf{P_a}$ established in the present work. The relative free energies are given in kcal mol^{-1}.

affecting the site-selectivity of these reactions were thoroughly investigated. We anticipate that these results will be informative for the future design of related catalytic reactions.

For the **1a** system, the DFT-computed free energy profiles are given in Fig. 1. The reaction is initiated by coordination of $KAuBr_4$ with the C···C bond of **1a** to give Au···π coordinated complex **IM1**. Then the **2M** N atom, acting as a nucleophile, attacks the alkyne internal C atom of **IM1** due to the greater electron-deficiency of the internal C over the terminal C, as indicated by the calculated NBO charges (0.385*e* for the former and −0.443*e* for the latter). Through **TS2-3**, the necessary Au(III) carbenoid **IM3** can then be formed by cleaving the N–O bond[7,8] with a barrier of 10.9 kcal mol^{-1}. From **IM3**, C^a nucleophilic attack at carbene C will exclusively produce product $\mathbf{P_a}$. Therefore, we firstly evaluated the direct attack mechanism.[9] Unexpectedly, the desired C^a-attack denoted as **TS3-9** is 3.7 kcal mol^{-1} less stable than the C^t-attack *via* **TS3-4**. Therefore, we explored a new mechanism, initiated by one Br(Au) migration. As shown in Fig. 1(black line), one Br(Au) transfers to the carbene C atom to give **IM5**. The calculations indicate that, through **TS3-5**, Br-migration occurs with a barrier of only 0.2 kcal mol^{-1} and is exergonic by 10.8 kcal mol^{-1}. Subsequently, an unprecedented "SN2-type N-donation/abstraction substitution" achieves a formal C^b-attack, in which the sp^2–N atom substitutes with the migrated-Br *via* **TS5-7** (N-donation substitution) and is then replaced by a C^b atom *via* **TS7-8** (N-abstraction substitution), affording the five-membered cyclized intermediate **IM8**. After ring expansion through the C(Au) migration to the C^a atom, the target C^a-attack complex **IM9** is obtained with an energy demand of 14.6 kcal mol^{-1} relative to **IM8**. From the formal C^a-attack pathway (black line), one can clearly see that three energetically comparable TSs leading to $\mathbf{P_a}$, **TS3-5**, **TS5-7**, and **TS7-8**, are lower in energy than **TS3-4** (red line) and **TS3-9** (blue line). Two crucial factors might be responsible for such energy differences. One is the extremely flat Br-migration due to much smaller structural deformation with slight change of the Br–Au–C(carbene) angle (see Fig. S1 in the ESI†). And the other may be related to the high stability of **IM5** after Br-migration, which remarkably reduces the potential energy surface of subsequent processes, making the formation of $\mathbf{P_a}$ easier. From **IM3**, other possible reaction scenarios are disfavoured energetically and are given in Fig. S2 of the ESI.†

Following **IM9**, the C^a-attached H atom transfers to the sp^2–N atom resulting in the formation of $\mathbf{P_a}$. The calculated results indicate that the (C^a)H firstly transfers to one adjacent (S)O atom of the Ts fragment and then is trapped by the sp^2–N atom with the assistance of KBr. The H-shift step *via* **TS9-10** surmounts an energy demand of 6.5 kcal mol^{-1} and affords the extremely exergonic intermediate **IM10** owning to the formation of the aromatic benzene ring.[10] **IM10** then experiences a KBr

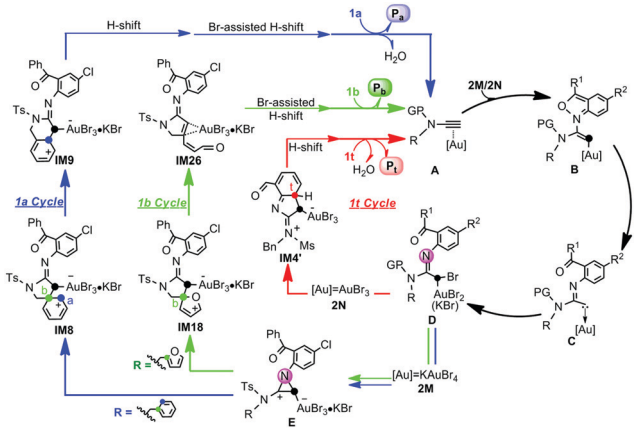

Fig. 2 Plausible catalytic cycles for the Au(III)-catalyzed selective annulations of *N*-aryl ynamides with anthranils based on the current calculations.

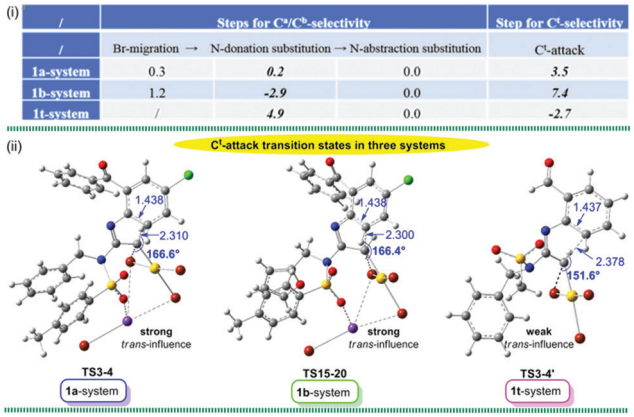

Fig. 3 (i) The relative free energies (in kcal mol^{-1}) for the crucial site-selective transition states, as well as (ii) optimized geometries with selected structural parameters for C^t substitution transition states in **1a**-/**1b**- and **1t**-systems. The bond distance and bond angle are given in Å and °, respectively.

Br-assisted H-abstraction/donation, smoothly giving rise to the target product $\mathbf{P_a}$ after dehydration. Along the reaction coordinate, the C^b-substitution by the N atom, corresponding to the **IM7** → **IM8** transformation, is considered as the rate-determining step of the whole reaction and has a barrier of 23.1 kcal mol^{-1}.

In the case of the **1b** annulation, the proposed mechanism of the **1a**-system, Au(III)-coordination → anthranil N nucleophilic addition → N–O cleavage → Br-migration → N-donation/abstraction substitution, is applied to rationalize the C^b-attack to the C(Au) atom for formation of key intermediate **IM18** (**1b** Cycle, Fig. 2). Then, the reaction is predisposed to chemoselectively cleave the C^b–O bond of the furan moiety *via* **TS18-24** to provide **IM26**. The alternative C(Au)-migration (**TS18-21**, Fig. S3, ESI†) was also examined and found to be highly unfavourable (−34.7 kcal mol^{-1} for **TS18-21** and −44.9 kcal mol^{-1} for **TS18-24**). With the C^b–O cleavage, the Br-assisted stepwise H-shift finally produces $\mathbf{P_b}$ and regenerates the KAuBr$_4$ active catalyst. Finally, the **1t** reaction mechanism was considered (**1t** Cycle, Fig. 2). After Au(III)-coordination, N nucleophilic addition, N–O cleavage and Br-migration,[11] C^t-substitution with Br(Au) is selectively favoured, from which the C^t-attached H-shift and subsequent dehydration, results in $\mathbf{P_t}$ formation. The calculated results for other competitive pathways involved in **1b**- and **1t**-systems are illustrated in Fig. S4 and S5 in the ESI.†

We then turned our attention to uncover how the nucleophilic site-selectivity at C^a, C^b and C^t atoms are controlled in these reactions. The relative free energies for the transition states (TSs) of key Br-migration, N-donation substitution and N-abstraction substitution leading to C^a/C^b selectivity, as well as that of C^t-attack resulting in C^t-selectivity are summarized in Fig. 3(i). Note that, in **1a**-/**1b**- and **1t**-systems, the N-donation substitution TSs (**TS5-7**/**TS16-17** and **TS3′-5′** in Fig. 1 and Fig. S4, S5, ESI†) exhibit very similar characteristics for the reaction regions with selected (sp^2)N···C(Au) distances of 1.934 Å, C(Au)···Br distance of ∼3.000 Å and (sp^2)N–C(N)–C(Au) angle of 89.6°. Intriguingly, compared with the N-donation substitution TSs, the competitive C^t-attack TSs exhibit almost opposite stability changes (0.2 *vs.* 3.5 in the **1a**-system, −2.9 *vs.* 7.4 in the **1b**-system and 4.9 *vs.* −2.7 kcal mol^{-1} in the **1t**-system, respectively).

Thus, it is predicted that the site-selectivity is closely related to the geometric constrains of the C^t-attack TS. The distinctive degree of the *trans*-influence of the Br atom is mainly responsible for the bifurcated selectivity at C^a/C^b and C^t atoms. It can be seen in Fig. 3 (ii) that a weaker *trans*-influence is exhibited in the **1t**-system with a Br–C(carbene)–C^t bond angle of 151.6° (166.6° in the **1a**-system and 166.4° in the **1b**-system), which, in turn, makes the interaction of the C^t with the C(carbene) atom easier. As a result, smaller energy demand is required for the **1t**-system. In contrast, because of the greater Br *trans*-influence, the resultant larger energy demand forces the **1a**- and **1b**-systems to follow the N-donation substitution and thus C^a/C^b selectivity is favoured.

After favourable N-donation substitution followed by N-abstraction substitution in the **1a**-/**1b**-systems, C^a- and C^b-selectivity was further evaluated. Two selective-determining TSs for the ring-expansion with C^a-selectivity and ring-opening with C^b-selectivity, **TS8-9** *vs.* **TS8-9′** in the **1a**-system and **TS18-21** *vs.* **TS18-24** in the **1b**-system, were compared and given in Fig. 4. For the **1b**-system, the main driving force for the favoured ring-opening might originate from the greater electrostatic O···C^2 interaction.[12] As shown by the calculated NBO charges, the charges on O and C^2 atoms in **TS18-24** are −0.45 and 0.39 e, whereas those of C(Au) and C^a in **TS18-21** are −0.42 and −0.18 e, respectively. Clearly, the stronger electrostatic attraction involved in **TS18-24** is more advantageous to cleave the C^b–O bond and thereby generates a relatively lower energy consumption. Nevertheless, significantly different from five-membered ring-opening in the **1b**-system, **TS8-9′** in the **1a**-system is characteristic of a six-membered ring-opening, in which the C^b–C^4 bond rupture will generate a substantially unstable terminal C cation, thereby resulting in a greater energy requirement. Consequently, the reaction is forced to follow a C^a-selective ring-expansion *via* **TS8-9**.

In summary, the mechanisms and origins of multiple nucleophilic site-selectivity of Au(III)-catalyzed annulations of substituted-anthranil **2M** with *N*-benzyl ynamide **1a** and *N*-furanylmethyl ynamide **1b**, as well as that of unsubstituted-anthranil **2N** and *N*-benzyl ynamide **1t**, have been elucidated

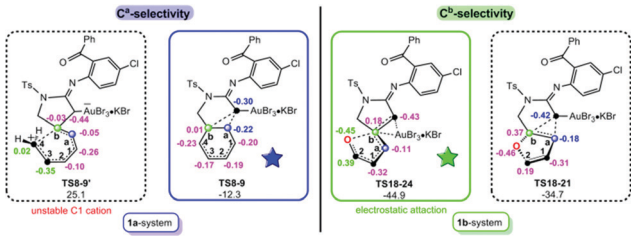

Fig. 4 The schematic structures with NBO charges (in e) for competitive C^a and C^b selective-determining transition states in **1a**- and **1b**-systems.

using DFT calculations. A unified and rational mechanism is presented in Fig. 2. After Au(III) coordination → **2M**/**2N** N nucleophilic addition → N–O cleavage to afford gold carbene intermediate **C**, further Br(Au)-migration affords a common bromide intermediate **D**. Then, the three competitive reaction sites, C^a, C^b and C^t, selectively attack the Au-attached C atom, resulting in the distinct products. For **1a**-/**1b**-annulations, a common key issue concerning a formal C^b-attack is established and involves an unprecedented "SN2-type N-donation/abstraction substitution" process. Subsequently, the reaction undertakes either C^a-migration → H-shift → Br-assisted H-shift → dehydration to form the C^a-attack product $\mathbf{P_a}$ in the **1a**-system or C–O cleavage → Br-assisted H-shift to furnish the C^b-attack product $\mathbf{P_b}$ in the **1b**-system. For $\mathbf{P_t}$ formation in the **1t** system, the bromide intermediate, undergoes selective C^t-substitution with Br(Au), C^t-attached H-shift and dehydration.

For these annulation reactions, the present study indicates that the strength or weakness of the Br(Au) *trans*-influence dominates the nucleophilic selectivity for the C^a/C^b or C^t atoms. Furthermore, the C^a site-selectivity in the **1a**-system can be attributed to the rather unstable terminal C cation in the ring-opening TS leading to C^b-attack, while the strong C···O electrostatic attraction in the crucial ring-expansion TS is responsible for the preferred C^b-selectivity in the **1b**-system. In summary, we anticipate that the controlling factors involved in the nucleophilic site-selectivity observed for these reactions can be applied to other transition metal carbene-promoted reactions.

This work was jointly supported by the National Natural Science Foundation of China (21873055), the Natural Science Foundation of Shandong Province (ZR2019MB016 and ZR20170 9240033), Key Laboratory of Emergency and Trauma (Hainan Medical University), Ministry of Education (KLET-201903). TDJ wishes to thank the Royal Society for a Wolfson Research Merit Award and the Open Research Fund of the School of Chemistry and Chemical Engineering, Henan Normal University for support (2020ZD01).

Conflicts of interest

There are no conflicts to declare.

Notes and references

1 (*a*) D. J. Gorin and F. D. Toste, *Nature*, 2007, **446**, 395; (*b*) R. Dorel and A. M. Echavarren, *Chem. Rev.*, 2015, **115**, 9028; (*c*) A. Furstner, *Chem. Soc. Rev.*, 2009, **38**, 3208; (*d*) L. Fensterbank and M. Malacria, *Acc. Chem. Res.*, 2014, **47**, 953; (*e*) L.-W. Ye, X.-Q. Zhu, R. L. Sahani, Y. Xu, P.-C. Qian and R.-S. Liu, *Chem. Rev.*, 2020, DOI: 10.1021/acs.chemrev.0c00348; (*f*) R. L. Sahani, L.-W. Ye and R.-S. Liu, *Adv. Organomet. Chem.*, 2020, **73**, 195; (*g*) E. Aguilar and J. Santamaría, *Org. Chem. Front.*, 2019, **6**, 1513.

2 (*a*) S. Hahn, S. Koser, M. Hodecker, P. Seete, F. Rominger, O. Miljanic, A. Dreuw and U. H. F. Bunz, *Chem. – Eur. J.*, 2018, **24**, 6968; (*b*) L. Ji, A. Friedrich, I. Krummenacher, A. Eichhorn, H. Braunschweig, M. Moos, S. Hahn, F. Geyer, O. Tverskoy, J. Han, C. Lambert, A. Dreuw, T. Marder and U. H. F. Bunz, *J. Am. Chem. Soc.*, 2017, **139**, 15968; (*c*) Z. Zeng, H. Jin, X. Song, Q. Wang, M. Rudolph, F. Rominger and A. S. K. Hashmi, *Chem. Commun.*, 2017, **53**, 4304.

3 (*a*) M.-H. Tsai, C. Wang, A. S. K. Raj and R.-S. Liu, *Chem. Commun.*, 2018, **54**, 10866; (*b*) R. L. Sahani and R. Liu, *Angew. Chem., Int. Ed.*, 2017, **56**, 1026; (*c*) R. L. Sahani and R.-S. Liu, *Angew. Chem., Int. Ed.*, 2017, **56**, 12736; (*d*) G. Ung, M. Soleilhavoup and G. Bertrand, *Angew. Chem., Int. Ed.*, 2013, **52**, 758.

4 Z. Zeng, H. Jin, M. Rudolph, F. Rominger and A. S. K. Hashmi, *Angew. Chem., Int. Ed.*, 2018, **57**, 16549.

5 H. Jin, L. Huang, J. Xie, M. Rudolph, F. Rominger and A. S. K. Hashmi, *Angew. Chem., Int. Ed.*, 2016, **55**, 794.

6 (*a*) A.-H. Zhou, Q. He, C. Shu, Y.-F. Yu, S. Liu, T. Zhao, W. Zhang, X. Lu and L.-W. Ye, *Chem. Sci.*, 2015, **6**, 1265; (*b*) L. Li, T.-D. Tan, Y.-Q. Zhang, X. Liu and L.-W. Ye, *Org. Biomol. Chem.*, 2017, **15**, 8483; (*c*) H. Li, J. Liu, A. A. Ogunlana and X. Bao, *Org. Chem. Front.*, 2017, **4**, 1130; (*d*) S. S. Giri and R.-S. Liu, *Chem. Sci.*, 2018, **9**, 2991.

7 A. A. Ogunlana and X. Bao, *Chem. Commun.*, 2019, **55**, 11127.

8 (*a*) K. Wang, Y. Liu, Q. Wu, L. Liu, Y. Li, T. D. James, G. Chen and S. Bi, *Mol. Catal.*, 2020, **480**, 110647; (*b*) Y. Liu, X. Yang, L. Liu, H. Wang and S. Bi, *Dalton Trans.*, 2015, **44**, 5354; (*c*) Y. Liu, K. Wang, B. Ling, G. Chen, Y. Li, L. Liu and S. Bi, *Catal. Sci. Technol.*, 2020, **10**, 4219.

9 (*a*) T. Li, W. Rong, T. Zhang and J. Li, *ChemCatChem*, 2020, **12**, 5276; (*b*) C. Zhu, L. Kou and X. Bao, *Chin. J. Chem.*, 2020, **38**, 57; (*c*) A. K. Sahoo, R. Vanjari, S. Dutta, B. Prabagar and V. Gandon, *Chem. – Asian J.*, 2019, **14**, 4828.

10 (*a*) M. J. Dewar, *Angew. Chem., Int. Ed. Engl.*, 1971, **10**, 761; (*b*) M. Randić, *Chem. Rev.*, 2003, **103**, 3449; (*c*) Z. W. Davis-Gilbert, X. Wen, J. D. Goodpaster and I. A. Tonks, *J. Am. Chem. Soc.*, 2018, **140**, 7267.

11 It is confirmed by the IRC calculations that, in the **1t**-system, the N–O bond breaks with simultaneous Br(Au)-migration, implying that the energy surface of the Br-migration is very flat. This fact can be indirectly corroborated by the corresponding step in the **1a**- and **1b**-systems, where the activation barriers are only 0.2 (Fig. 1) and 0.7 kcal mol^{-1} (Fig. S4, ESI†), respectively.

12 In addition, to examine the contribution of the O···C^2 electrostatic attraction to O–C^b cleavage, the furan O atom is replaced by a C atom (Fig. S6, ESI†). It was found that the ring-opening transition state is 2.8 kcal mol^{-1} higher in energy than the ring-expansion transition state, indicating that a strong electrostatic attraction between the O and C^2 is a factor in the C^b-selectivity.

